Oil Shale, 2015, Vol. 32, No. 1, pp. 5–24
doi: 10.3176/oil.2015.1.02
ISSN 0208-189X

PALEOLIMNOLOGICAL ENVIRONMENTS AND ORGANIC ACCUMULATION OF THE NENJIANG FORMATION IN THE SOUTHEASTERN SONGLIAO BASIN, CHINA

HANSHENG CAO[(a)], WEI GUO[(a)]*[*], XUANLONG SHAN[(a)], LIN MA[(b)], PINGCHANG SUN[(a)]

[(a)] College of Earth Sciences, Jilin University, Changchun 130061, China
[(b)] School of Earth, Atmospheric and Environment Science, University of Manchester, M13 9WJ Manchester, UK

Abstract. *Thick layers of dark lacustrine mudstone in the Nenjiang Formation record the evolution of local depositional environments in the Songliao Basin. This evolution in lake water is accurately reflected in variations in trace element compositions in sedimentary rocks. In this study, element geochemistry and clay mineralogy in successive cores were investigated to have a closer insight into the paleolimnological environment and organic accumulation during the Nenjiang epoch. Analysis of the contents of Mn, Ca and Ti, as well as Rb/Sr and Sr/Cu revealed that paleoclimate cycled between warm and humid to semi-arid and hot. The study of Sr/Ba ratios, clay minerals and stable isotopes indicated that both high and low salinity existed in two stages, and that high salinity in Member 1 of the Nenjiang Formation is likely correlated with transgressive events. Analysis of the ratios of V/V + Ni, Ni/V and Th/U suggested that the paleolimnological environment was reducing. The investigation of paleotemperature demonstrated that the Nenjiang Formation was deposited in a warm water environment, analysis of carbon and oxygen isotopes revealed its deposition in open paleolake. High paleoproductivity and salinity as well as redox potentials represent the most favorable environment for oil shale enrichment.*

Keywords: *Nenjiang Formation, paleoclimate, paleosalinity, redox conditions, paleolimnological characteristics, enrichment of oil shale.*

1. Introduction

Dark mudstone is widely and abundantly distributed in the Nenjiang Formation of the Songliao Basin, NE China. Stable, deep and semi-deep lake sediment facies have developed, while tectonic activity was weak during the

* Corresponding author: e-mail *365683460@qq.com*

Nenjiang epoch in this area. As a result, the immature dark mudstone contains abundant paleolimnological information. The layers in these rocks reach 84 m in thickness, and the total thickness is as much as 289 m in the Shen Jingzi area. Previous studies addressed in more detail the sedimentary sequence, paleontology and trace elements to inverse the paleolimnological conditions, and were mostly based on a single factor to conduct [1–5]. In addition, the controversy related to the marine incursion event in the Late Cretaceous Songliao Basin never stopped [6, 7]. By the integrating of major and trace as well as isotope elements and clay minerals analyses in high resolution, in this paper the limnological environments could be reconstructed more effectively, supporting evidence for transgression and laying the foundation for the enrichment regularity of organic matter.

2. Geological setting

The Songliao Basin, located in northeastern China, is about 260,000 km^2 in area [8]. This Meso-Cenozoic, large and composite sedimentary basin with fault-depression dual structure represents an essential oil and gas production base in China. Based on the basement and regional geological characteristics of the caprock, it can be divided into six first-order tectonic units: the Western Slope, the Southwestern Uplift, the Southeastern Uplift, the Central Depression, the Northeastern Uplift and the North Plunge (Fig. 1). The 36,000 m^2 Northeastern Uplift Zone underwent an early syn-rift depression, the post-rifting thermal depression and the late post-rifting shrinkage [9]. The tectonic evolution controlling dynamics was primarily derived from thermodynamic energy in magmatic complexes from the deep crust, subduction from the Transpacific to the Paleo-Asian plate and the closure of the Sea of Okhotsk [10].

The basement of the Songliao Basin is a continental crust formed in the Late Paleozoic – Early Mesozoic, and primarily comprises Carboniferous-Permian metamorphic rocks and magmatic rocks of the same period. The sedimentary cover in the basin is composed of Mesozoic-Cenozoic strata. The total thickness of the basement is more than 10 km [9, 10]. After the Deng Louku Formation of Lower Cretaceous was formed, extensive subsidence took place in the Southeastern Uplift Zone. As a result, the Lower Cretaceous Quantou Formation and the Upper Cretaceous Qing Shankou, Yaojia and Nenjiang Formations were developed in the depression period, predominantly composed of terrigenous clastic rocks of fluvial and lake facies. The basin's largest, Nenjiang Formation, is divided into five subsections. During the deposition of Member 2 of the Nenjiang Formation, the lake area reached the maximum and deposited a thick succession of dark mudstone.

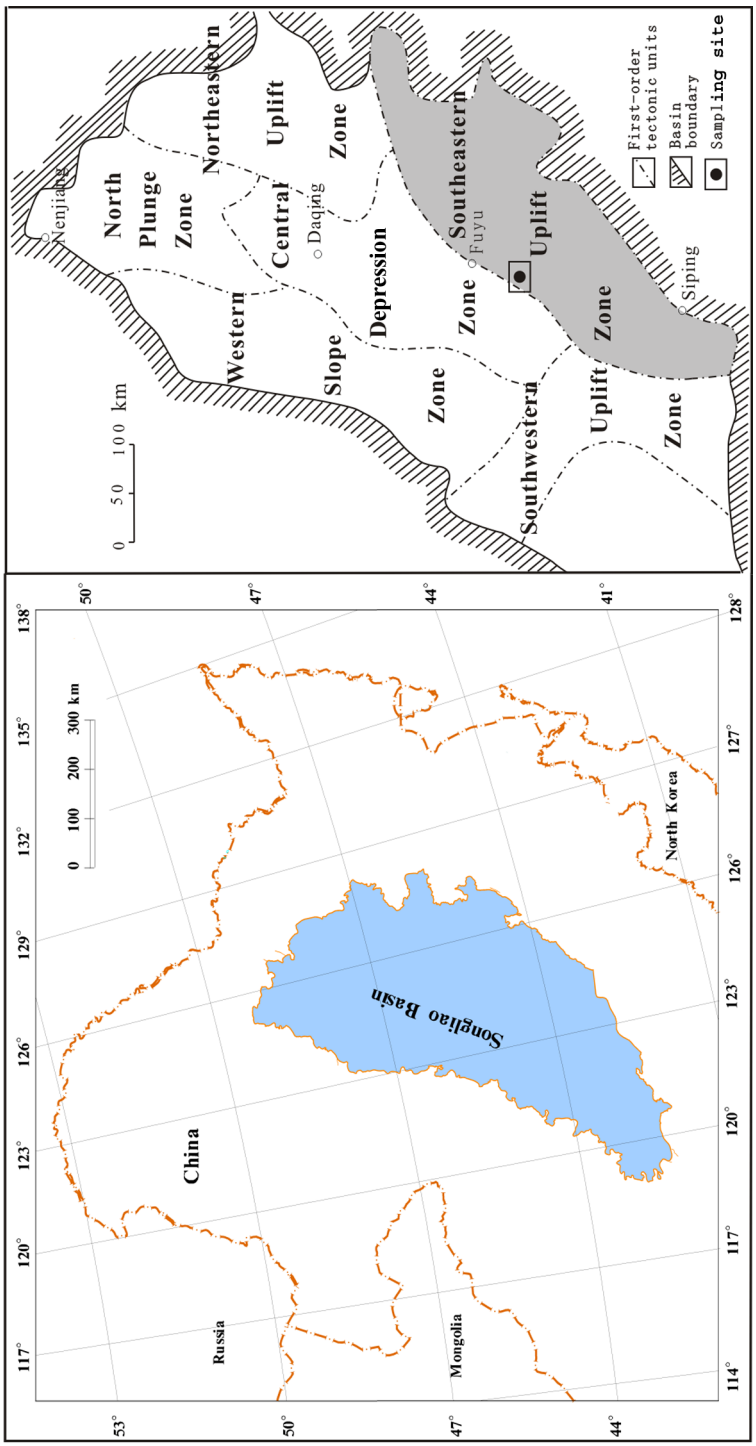

Fig. 1. Location of the Songliao Basin and the sampling site.

3. Materials and methods

3.1. Collection of samples

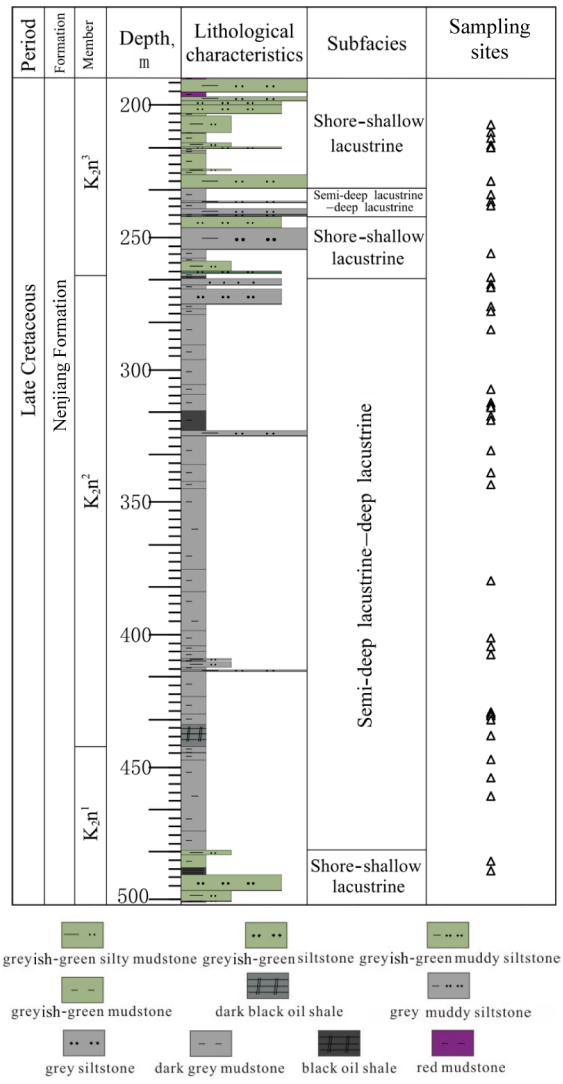

Fig. 2. Lithologic log of the ZK1489 drill core of the Nenjiang Formation and sampling points, Songliao Basin.

Based on comprehensive studies of outcrops and trenches, and a detailed description of various boreholes in the Shen Jingzi section in the Southeastern Uplift Zone, it was revealed that the Nenjiang Formation was deposited in a stable depositional environment. Samples were taken from the fully cored well ZK1489, with a total depth of 500 m. Well ZK1489 was selected as it represents the typical evolution of depositional environment. The samples of the Nenjiang Formation are fresh, with no calcite veins or fractures (Fig. 2). Oil shale at the base of Nenjiang Member 1 and Nenjiang Member 2 is 8 m and 7.5 m thick, respectively.

3.2. Analytical methods

The abundances of 31 elements were measured by ICP-MS and X-ray fluorescence spectrometry, of which 11 with environmental significance were chosen for further study. These included Mn, Ca, Ti, Sr, Ba, Rb, Cu, V, Ni, Th and U. Carbon and oxygen isotopes were analyzed at the Beijing Geological Institute (Beijing, China). The abundance of clay minerals was measured by the x-ray diffraction (XRD) in model of D/mas rAX in the Oil Shale Test Center of Jilin University (Changchun, China). Every scanning interval by Cu-Ka rays is 0.04° and 2S, and scanning range is 2°–60°2θ. The

relative content is calculated according to the spectra which are analyzed by the time of appearance of minerals and the corresponding peak area. Appropriate analysis materials include biological fossils or carbonate minerals. Accordingly, we selected ostracodes, bivalves and conchostracans, fossilized in argillaceous rocks for microscope and scanning electron microscope observation. Carbon and oxygen isotope compositions were measured by the phosphoric acid method by employing a MAT-253 mass spectrometer (Finnigan Company, Germany) and the final results were calibrated according to PDB standards (the PDB scale refers to the isotopic compositions of elements in calcite).

3.3. Depositional characteristics of drill core

On the basis of core and field profile observation and systematic geochemical testing, sedimentary facies is mainly lacustrine in this area. During deposition of the lower part of Member 1 of the Nenjiang Formation, the greyish-green siltstone interbedded with silty mudstone and mudstone developed in shore-shallow lake facies were deposited in the lake. During deposition of the upper Nenjiang Member 1 and Nenjiang Member 2, dark grey-grey mudstone and shale with interbedded grey silty mudstones were deposited in semi-deep and deep lakes following the lake expanding and deepening. The abundant carbonaceous plant fragments were witnessed in some dark mudstones (Fig. 3a). Horizontal bedding was widely developed in the sediment of mainly mudstone and deformed beds and shearing tectonic activity were found as well. The gravity flows deposit occurred at a depth of 447 m (Fig. 3b). Furthermore, large quantities of ostracoda, bivalves and conchostracans were observed in some sections (Fig. 3c). The Nenjiang Member 3 was characterized by the presence of greyish-green silty mudstone and siltstone interbedded with greyish-green mudstone, developed in a semi-deep lacustrine to shore-shallow lake. Red mudstone was deposited at the top, reflecting the gradual decrease of water depth.

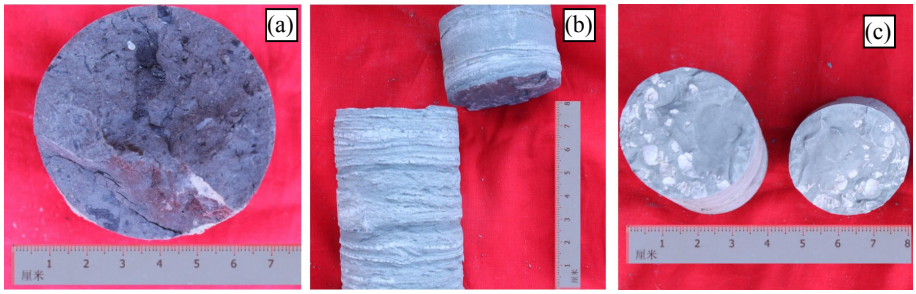

Fig. 3. Sedimentary structures and paleontological features of the Nenjiang Formation in the Southeastern Uplift Zone, Songliao Basin: (a) abundant Carbonaceous plant fragments in mudstones, 256.6 m, K^2n^2; (b) sediment gravity flow, 447 m, K^2n^1; (c) bivalve fragments in light grey mudstone, 233.4 m, K^2n^3.

4. Results

4.1. Element geochemistry

The Ca content in the Nenjiang Formation ranged from 5192.97 to 190762.16 ppm with a mean of 35536.71 ppm, that of Mn from 112.76 to 4130.17 ppm with a mean of 668.01 ppm. The concentration of Ti was between 1679.31 and 4343.83 ppm with a mean of 3338.79 ppm (Table 1).

The ratio of Sr/Cu ranged from from 2.94 to 23.59 with a mean of 9.34, that of Rb/Sr from 0.10 to 0.69 with a mean of 0.43. The Sr/Ba ratio varied from 0.81 to 4.55 with a mean of 1.76, that of V/V + Ni from 0.50 to 0.82 with a mean of 0.72. Ni/V was from 0.22 to 1.00 with a mean of 0.40 and Th/U ratios ranged from 0.24 to 1.49 with a mean of 0.70 (Table 1).

Table 1. Major and trace element abundances (ppm) and ratios in mudstone rocks of the Nenjiang Formation

Sample	Depth, m	Ca	Mn	Ti	Sr/Cu	Rb/Sr	Sr/Ba	V/V+Ni	Ni/V	Th/U
ZK1489-86	197.63	20351.20	252.45	3252.77	11.86	0.44	1.20	0.70	0.43	0.96
ZK1489-82	207.36	30727.61	299.55	3446.58	11.58	0.39	1.59	0.74	0.35	0.51
ZK1489-81	210.55	15450.37	289.21	3187.59	8.68	0.57	1.05	0.70	0.42	0.56
ZK1489-80	212.55	13775.92	124.81	3495.51	6.48	0.56	0.97	0.75	0.33	0.56
ZK1489-72	228.85	21261.87	1470.61	3821.92	8.43	0.51	1.32	0.69	0.44	1.49
ZK1489-71	233.90	20440.19	161.18	3823.49	9.98	0.42	1.19	0.68	0.47	0.76
ZK1489-70	236.55	41941.32	226.83	3839.51	14.90	0.34	0.83	0.71	0.40	0.51
ZK1489-69	237.95	20632.48	112.76	3338.57	16.87	0.41	1.39	0.75	0.33	0.76
ZK1489-62	256.13	12941.34	297.11	3989.89	8.99	0.43	1.47	0.82	0.22	0.46
ZK1489-57	265.12	25647.01	879.89	3714.09	6.65	0.44	1.03	0.70	0.44	0.60
ZK1489-55(2)	267.80	18068.36	317.57	3297.28	2.94	0.47	2.25	0.76	0.32	0.41
ZK1489-55(1)	268.80	11586.74	896.68	3947.70	8.56	0.48	1.03	0.77	0.29	0.83
ZK1489-53	276.13	11006.28	620.75	4318.57	6.42	0.55	1.24	0.75	0.33	0.68
ZK1489-52	278.03	21589.12	524.54	3982.06	7.43	0.47	1.07	0.70	0.43	0.93
ZK1489-51	284.70	17990.68	838.90	4343.83	6.33	0.54	1.07	0.71	0.41	0.58
ZK1489-48	307.40	28394.71	137.42	4290.06	7.03	0.41	1.21	0.80	0.25	1.06
ZK1489-47	312.40	24628.54	436.62	3767.92	8.32	0.46	1.14	0.70	0.43	1.14
ZK1489-46	313.55	15365.42	1445.09	3628.36	4.79	0.46	0.90	0.73	0.37	1.33
ZK1489-45	314.35	7210.32	275.00	3882.49	7.17	0.53	1.44	0.80	0.24	0.82
ZK1489-41(2)	317.55	67448.35	1206.19	2981.38	11.45	0.46	1.80	0.66	0.52	1.04
ZK1489-40	319.15	20940.68	195.06	3628.50	8.81	0.38	2.28	0.73	0.37	0.72
ZK1489-36	343.37	28366.41	2183.93	3084.81	5.83	0.43	0.81	0.55	0.82	1.08
ZK1489-34	379.65	16102.10	228.81	3354.65	9.19	0.53	1.48	0.71	0.40	0.54
ZK1489-32	401.25	6498.85	864.90	3057.23	5.32	0.61	1.41	0.77	0.30	0.55
ZK1489-30(2)	404.41	28064.11	409.87	3573.83	8.71	0.53	1.33	0.75	0.33	0.47
ZK1489-30(1)	407.58	5192.97	785.15	2588.94	3.59	0.62	1.61	0.79	0.26	0.58
ZK1489-21	429.20	13563.65	463.26	3511.38	3.65	0.63	2.15	0.82	0.22	0.80
ZK1489-19(1)	429.55	8814.60	242.59	3438.17	5.64	0.48	1.24	0.74	0.35	0.79
ZK1489-17	429.90	70353.04	438.65	2460.65	3.69	0.35	1.42	0.78	0.29	0.35
ZK1489-16	430.60	9644.85	172.56	3926.21	7.14	0.45	0.92	0.79	0.26	0.86
ZK1489-15	432.00	71110.97	463.26	2688.38	13.93	0.19	3.58	0.77	0.31	0.49

Table 1. (Continued)

Sample	Depth, m	Ca	Mn	Ti	Sr/Cu	Rb/Sr	Sr/Ba	V/V+Ni	Ni/V	Th/U
ZK1489-14	438.20	6771.24	140.14	3700.90	3.18	0.69	4.10	0.74	0.35	0.49
ZK1489-11	447.15	141059.02	941.25	2069.54	16.70	0.15	2.09	0.50	1.00	0.74
ZK1489-10(2)	454.00	39158.67	341.54	2798.94	15.98	0.31	4.55	0.77	0.31	0.44
ZK1489-10(1)	460.80	36406.28	213.65	2725.15	6.32	0.31	2.80	0.75	0.33	0.75
ZK1489-6	485.42	190762.16	4130.17	1679.31	17.58	0.19	3.25	0.53	0.88	0.61
ZK1489-5	489.17	96432.80	1591.97	2138.76	21.27	0.14	4.34	0.62	0.61	0.24
ZK1489-3	493.46	114694.81	764.54	2099.20	23.59	0.10	2.22	0.69	0.45	0.29
Mean		35536.71	668.01	3338.79	9.34	0.43	1.76	0.72	0.40	0.70
Median		20786.58	423.25	3471.05	8.38	0.46	1.40	0.74	0.35	0.65
Max		190762.16	4130.17	4343.83	23.59	0.69	4.55	0.82	1.00	1.49
Min		5192.97	112.76	1679.31	2.94	0.10	0.81	0.50	0.22	0.24

4.2. Clay minerals

The XRD data presented in Table 2 show that the terrigenous detrital minerals of mudstone rocks are mainly quartz, feldspars and plagioclase, with the average contents of 36.44%, 7.33% and 10.39%, respectively. The endogenous chemical sediments are mainly calcite and dolomite, with the average contents of 4.78% and 1.56%, respectively. There exist two kinds of

Table 2. The relative clay mineral content of mudstone rocks of the Nenjiang Formation

Sample	Relative content of clay mineral, /10^{-2}									
	Q	FE	PL	CA	DO	SI	PY	ILSM	IL	KA
ZK1489-80	37.00	6.00	9.00	3.00				14.00	22.00	9.00
ZK1489-70	40.00	11.00	18.00	4.00					22.00	5.00
ZK1489-62	46.00	8.00	16.00					4.00	18.00	8.00
ZK1489-55	39.00	10.00	8.00				3.00	8.00	24.00	8.00
ZK1489-53	47.00	8.00	11.00					10.00	16.00	8.00
ZK1489-51	33.00	7.00	9.00	3.00		4.00		9.00	28.00	7.00
ZK1489-48	40.00	7.00	10.00	4.00				8.00	25.00	6.00
ZK1489-41	36.00	5.00	7.00	5.00	12.00			11.00	24.00	–
ZK1489-40	43.00	7.00	11.00	4.00				11.00	24.00	–
ZK1489-38	38.00	7.00	10.00					12.00	33.00	–
ZK1489-37	38.00	7.00	14.00					10.00	26.00	5.00
ZK1489-36	28.00	6.00	7.00			20.00		10.00	21.00	8.00
ZK1489-35	32.00	8.00	10.00	10.00				9.00	25.00	6.00
ZK1489-34	40.00	8.00	11.00					11.00	23.00	7.00
ZK1489-21	31.00	7.00	10.00	7.00			2.00	13.00	30.00	0.00
ZK1489-11	28.00	7.00	11.00	9.00	16.00		2.00		23.00	4.00
ZK1489-10	34.00	8.00	9.00	8.00				13.00	28.00	–
ZK1489-6	26.00	5.00	6.00	29.00			3.00	15.00	16.00	–
Average	36.44	7.33	10.39	4.78	1.56	1.33	0.56	9.33	23.78	4.50

Abbreviations used: Q – quartz; FE – feldspars; PL – plagioclase; CA – calcite; DO – dolomite; SI – siderite; PY – pyrite; ILSM – illite smectite; IL – illite; KA – kaolinite.

heavy minerals, namely siderite and pyrite, with an average content of 1.33% and 0.56%, respectively. Clay minerals are mostly composed of illite, with an average content of 23.78%, followed by illite smectite and kaolinite, with the average contents of 9.33% and 4.50%, respectively. The clay minerals account for about 37.61% of the whole rocks.

4.3. Carbon and oxygen isotopes

Stable isotope analysis is widely used to distinguish depositional environments. Compared with trace element analysis, it gives more reliable data, especially when there are rocks of different origin involved. 11 samples were analyzed for carbon and oxygen isotopes (Table 3). $\delta^{13}C$ ranged from –11.5 to 3.1‰ with a mean of –3.17‰ and $\delta^{18}O$ contents ranged from –10.6 to –7.3‰ with a mean of –9.05‰.

Table 3. C and O isotopes content of mudstone rocks of the Nenjiang Formation

Sample	Horizon	Lithology	Depth, m	$\delta^{13}C$, ‰	$\delta^{18}O$, ‰
ZK1489-87	K_2n^3	Reddish-brown mudstone	195.98	–3.9	–9.9
ZK1489-84	K_2n^3	Greyish-green siltstone	201.6	–11.1	–10.2
ZK1489-81	K_2n^3	Reddish-brown mudstone	210.55	–11.5	–7.3
ZK1489-72	K_2n^3	Greyish-green silty mudstone	228.85	–4.8	–9.5
ZK1489-62	K_2n^3	Grey argillaceous siltstone	256.13	–2.1	–10.6
ZK1489-40	K_2n^2	Black mudstone	345.4	2.9	–8.5
ZK1489-36	K_2n^2	Dark grey mudstone	343.37	2	–8.7
ZK1489-24	K_2n^2	Dark grey mudstone	418.68	–4.1	–7.8
ZK1489-14	K_2n^2	Greyish-black mudstone	438.2	0.1	–8.5
ZK1489-10	K_2n^1	Dark grey mudstone	447.3	3.1	–9.1
ZK1489-1	K_2n^1	Reddish-brown siltstone	500.50	–5.5	–9.5

5. Discussion

5.1. Indicators of paleoclimate

Ca, Mn and other chemical elements are deposited in lakes, rivers and terrigenous debris with precipitation. When rainfall exceeds evaporation, the ion concentrations of Ca and Mn are low enough for the elements to be deposited in the formation in low amounts. This suggests warm and humid climatic conditions during deposition. On the contrary, the high concentrations of Ca and Mn indicate hot and arid climatic conditions. Changes in the content of Ti reflect the degree of terrigenous debris input, with a positive correlation between the two. Higher concentrations of Ti suggest warm and humid conditions during deposition [11]. The Rb/Sr and Sr/Cu ratios in lake sediments are highly positive and serve as indicators of paleoclimate changes. Sediments usually display high Rb/Sr and low Sr/Cu ratios in warm and humid climatic conditions. The opposite pattern suggests hot, arid and low weathering rate climatic conditions during deposition [12].

The vertical variations of Ca, Mn and Ti contents, and Sr/Cu and Rr/Sr ratios with paleoclimate are shown in Figure 4. In this paper, we used Ward's clustering method and the Q-type factor analysis to classify paleoclimate data. Data processing measurement was done using the Squared Euclidean distance. In case of the five paleoclimate conditions, the correlation coefficient of Sr/Cu and Rr/Sr is the highest, 0.61. So, one parameter can be used in place of the other. Three types of paleoclimate data can be distinguished (Table 4). Based on cluster analysis results, the paleoclimate conditions in the Nenjiang Formation can be divided into five stages (Fig. 4). Stage 1 includes climate types I, II and III and shows an obvious trend of climate change from arid hot, semi-arid and hot towards warm and humid. Especially the early stage 1 experienced several climatic cycles, indicating unstable climate changes in the transition stage from the Nenjiang Member 1 to Member 2. On the whole, however, the climate changed warm and humid. In the middle Nenjiang Member 2 (stage 2) and the early Nenjiang Member 3 (stage 3), different element values and ratios reflected the change

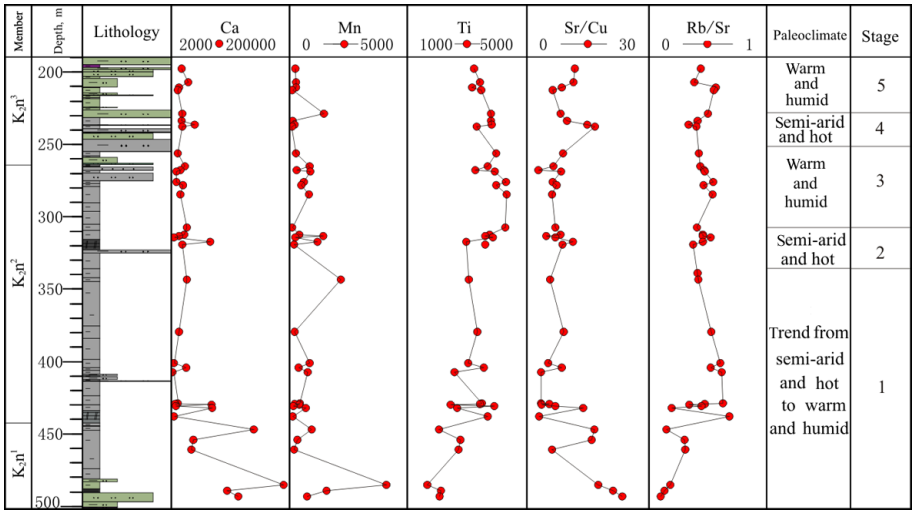

Fig. 4. Vertical changes of element contents and ratios with paleoclimate during deposition of the Nenjiang Formation.

Table 4. Results of cluster analysis of paleoclimatic indicators of the Nenjiang Formation

Climate type	Ca			Mn			Ti			Sr/Cu		
	Max	Min	Avg	Max	Min	Avg	Max	Min	Avg	Max	Min	Avg
I	190762	96433	135737	4130.2	785.2	1862.2	2798.9	2009.2	2284	23.59	16.7	19.7
II	71111	57189	66997	1206.2	247.5	525.16	3628.5	2460.7	2928.9	13.93	3.69	9.30
III	67448	5193	20286	2183.9	63.1	495.01	4343.8	1679.3	3449.9	16.87	2.94	8.02

of climate to semi-arid and hot, which corresponds to climate type II. As indicated by element analysis, in stages 3 and 5 warm and humid climate conditions predominated, corresponding to climate type III.

5.2. Indicators of paleosalinity

Sr and Ba are two elements with different rate of immigration following changes in paleosalinity. Sr/Ba ratio is widely regarded as an indicator of paleosalinity. The high Sr/Ba ratio reflects a high salinity in the ambient water, and the low ratio, a low salinity [13]. According to the vertical variation, paleosalinity is divided into four stages (Fig. 5). The Sr/Ba value ranges between 0.92 and 4.33 in the first stage, indicating a high salinity condition. The low Sr/Ba ratio reflects a decreased salinity in the second and fourth stages, respectively. In the middle Nenjiang Member 2, the Sr/Ba value (avg 1.85) also mirrors a high salinity condition in the third stage.

Many researchers have reconstructed paleosalinity and paleotemperatures through analysis of carbon and oxygen isotopes. The $\delta^{13}C$ level in carbonate minerals generally increases with increasing salinity [14]. Although isotopes in sediments exchange due to sedimentation or outside influences, this is not the case with carbon isotopes. $\delta^{18}O$ in carbonate also increases with increasing salinity caused by evaporation [15], but it is more sensitive to isotope exchange by sedimentation. In such instances a combined method of analysis of carbon and oxygen isotopes is more reliable.

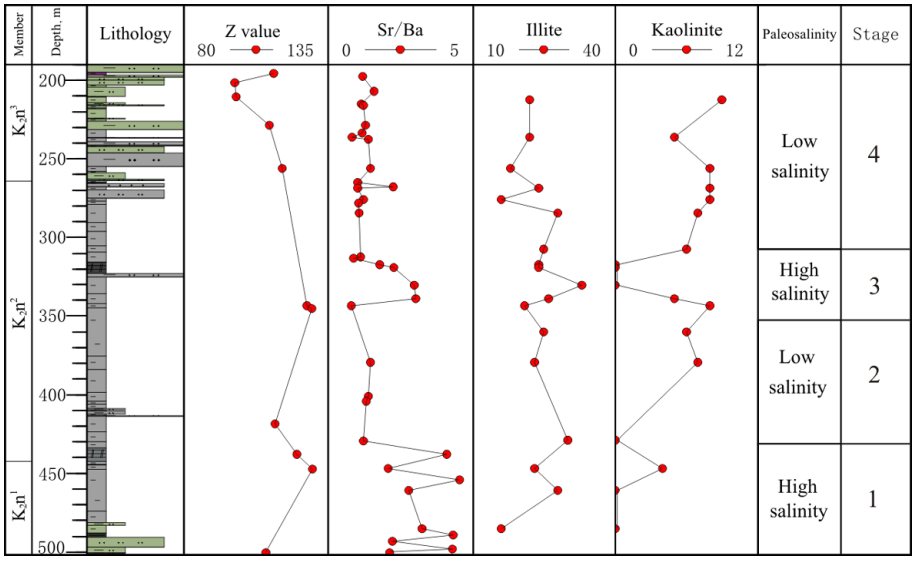

Fig. 5. Vertical changes of the relative paleosalinity of lake waters during deposition of the Nenjiang Formation.

Based on the formula $Z = 2.048*(\delta^{13}C + 50) + 0.498*(\delta^{18}O + 50)$, where Z represents paleosalinity, carbon and oxygen isotopes can be analyzed together to indicate relative paleosalinity [15]. A value of $Z > 120$ suggests the presence of marine deposits, while $Z < 120$ implies the presence of fresh water deposits (relative to the PDB standard). The calculated Z values of isotopes are given in Table 5. In general, paleosalinity exhibits a high-low-high-low trend of change and has two peak values, respectively (Fig. 5). We can conclude that the change of the Sr/Ba ratio is consistent with changes in paleosalinity.

Table 5. Calculated Z values of isotopes

Depth, m	195.98	201.6	210.55	228.85	256.13	345.4	343.37	418.68	438.2	447.3	500.5
$\delta^{13}C$（PDB）	–3.9	–11.1	–11.5	–4.8	–2.1	2.9	2	–4.1	0.1	3.1	–5.5
$\delta^{18}O$（PDB）	–9.9	–10.2	–7.3	–9.5	–10.6	–8.5	–8.7	–7.8	–8.5	–9.1	–9.5
Z value	114.4	99.5	100.1	112.8	117.7	129	127.1	115	123.3	129.1	111.3

Moreover, the Sr/Ba values in the first and third stages of salinity are higher than 120 and are indicative of the presence of the characteristics of marine deposits in these stages.

Clay minerals are also sensitive to depositional environment. Paleoclimate may have been controlled by difference between paleosalinity and salinity of water rich in certain ions [16]. Obviously, paleosalinity was the most important factor to influence the abundance of clay minerals. As salinity increased, first kaolinite was formed followed by illite and smectite [17]. Abundant illite and chlorite, and low content of kaolinite indicate a high salinity, while abundant kaolinite and low content of illite and chlorite, in contrast, suggest a low salinity [16–18].

In the first stage, the increasing content of illite and low abundance of kaolinite imply a high salinity. In the second stage the illite content shows a decreasing trend and that of kaolinite, an increasing trend, proving a low salinity. There is a peak value of illite content and a rapidly declining content of kaolinite in the third stage that also suggests a high salinity. The last, fourth stage represents a low salinity with low illite and high kaolinite contents. These trends are consistent with the results of element geochemistry and stable isotopes analysis.

Usually, hot and arid climatic conditions can enhance water evaporation, further resulting in a high salinity of water column. Compared with the first stage of paleoclimate, we found that the characteristics of high salinity in the first stage do not match with the trends of climate change from arid towards humid. In addition, in the Nenjiang Member 1 to the lower Nenjiang Member 2, the sedimentary environment changes from a shallow lake to a semi-deep lake environment, reflecting the process of deepening of water. This is also in contradiction with the process pattern following increase in salinity. Previous researches have shown that two large-scale marine trans-

gressions originated from the East-Asian Paleosea during the early Senomanian stage and the late Turonian to early Senonian stage in the Songliao Basin [11]. Furthermore, some evidences of paleontology indicate that the Songliao Basin undwerwent at least eight times the intermittent sea intrusion during the Nenjiang Member 1 to Member 2 epochs [19]. As a result, the Nenjiang Formation experienced the salinization of lacustrine water and developed a brackish water environment. Meanwhile, in well ZK1489 a wide area of lake sediments was found. This confirmed that the well was located near the center of the lake basin, which was thus less affected by provenance [20]. Therefore, the high salinity in the first stage was not due to paleoclimate or provenance, but was, in our opinion, more likely caused by transgression.

In its second and fourth stages, salinity was favoured by the extrapolated paleoclimate characteristics, in relatively hot and arid climate conditions paleosalinity was higher and in relatively humid climate conditions paleo-salinity was lower. In addition, we found that the third stage is different from the first one in course, which is also controlled by the paleoclimatic factors. Although in the lower Nenjiang Member 3 the paleoclimate became semi-arid and hot, the paleosalinity obviously did not increase due to the shrinkage of the basin and the increase of terrigenous supply. This resulted in the reduction of the water volume of the basin and the amount of salt precipitation.

5.3. Indicators of redox properties

The ratios of V/V + Ni, Ni/V and Th/U are often used as geochemical indicators of the redox properties of the ambient water. Typically, the high V/V + Ni ratio reflects reducing conditions, while Ni/V and Th/U decrease with increasing reductive capacity of depositional environments. Usually, the V/V + Ni > 0.54 reflects a reducing sedimentary environment, while the ratio ranging from 0.46 to 0.54 mirrors a neutral environment with relatively low oxygen levels, and the ratio < 0.46 suggests an oxidizing environment [21]. The average V/V + Ni ratio in argillaceous rocks was 0.72, with only one sample exhibiting ratios ranging from 0.46 to 0.54, the respective values of all other samples being higher (Fig. 6). This indicates the existence of a reducing environment in the Nenjiang Formation. Typically, the Ni/V ratio < 0.5 gives evidence of a reducing environment [21]; the average Ni/V in this study was 0.41, with only seven samples exhibiting ratios higher than 0.5. The Th/U ratio > 1.3 indicates an oxidizing environment, while the range of 0.8 to 1.3 reveals a weakly reducing environment, and the ratio < 0.8 implies a reducing environment [21]. In this study, the average ratio of Th/U was 0.71, while 11 samples exhibited ratios ranging from 0.8 to 1.3. These results show that the Nenjiang Formation was deposited in a reducing, deeply lacustrine environment, although the reductive strengths demonstrated some variation. This suggests that the conditions at the lake bottom changed little in terms of redox characteristics.

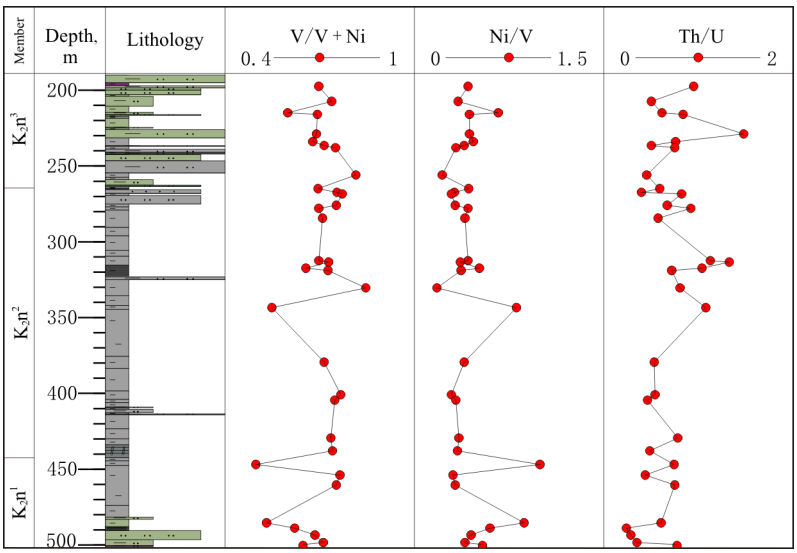

Fig. 6. Vertical changes of redox properties in the Nenjiang Formation.

5.4. Paleotemperature of water

Water temperature plays an important role in stabilizing carbonate isotopes, and has a greater effect on $\delta^{18}O$ content than does salinity. Temperature-influenced segregation effects on oxygen isotopes in calcite or fossilized shells were 0.26% per degree Celsius [22]. However, the effect of temperature on carbon isotopes was only 0.035%/°C [23]. This suggests that temperature has a significant effect on segregation in oxygen isotopes, but not on carbon isotopes. When carbonate was in equilibrium with water medium, $\delta^{18}O$ contents decreased with increasing temperature [24]. It is known that latitude affects $\delta^{18}O$ content, which is close to zero near the equator, and gradually decreases at higher latitudes, becoming negative. The latitude effect in the study region is about –0.21‰ [25]. The paleolatitude of the Songliao Basin ranged from 38 to 47° in the Cretaceous [26]. We extrapolated the locations of drilling cores to be at a paleolatitude of about 42°. The $d^{18}O_w$ value was calculated to be –8.82‰ (–0.21 × 42 = –8.82‰) in the Songliao Basin. Using the following two empirical formulas, we calculated the paleotemperature values [27]:

$$t = 16.9 - 4.2\,(\delta'c - \delta'w) + 0.13\,(\delta'c - \delta'w)^2 \quad (1)$$

$$t = 19.0 - 3.52\,(\delta'c - \delta'w) + 0.03\,(\delta'c - \delta'w)^2, \quad (2)$$

where t refers to the paleotemperature of water, °C; δ′c denotes the $\delta^{18}O$ value in CO_2 released from calcium carbonate treated with 100% phosphoric acid at 25 °C (αco_2-calcite = 1.01025); δ′w signifies the δ^{18} O value of CO_2 when solid carbonate is in equilibrium with dissolved carbonate (αco_2-H_2O = 1.0412). The estimated error of the $\delta^{18}O$ measured with a MAT-253 mass spectrometer is ± 0.06‰ and that of the calculated temperature is ± 0.27‰.

Calculations showed that the paleotemperature ranged from 12.27 ± 0.27 to 25.07 ± 0.27 °C in the Nenjiang Formation, with a mean of 18.9 ± 0.27 °C (Table 6). This suggests that the Nenjiang Formation was generally deposited in a warm environment. Deposition occurred in deep water mostly in Nenjiang Members 1–3, which does not directly represent the atmospheric temperature. As shown in Table 6, the paleotemperature during the Nenjiang Member 1–2 epochs were significantly lower than in the Nenjiang Member 3. As the paleotemperature is primarily affected by water depth and latitude, no significant changes occur within a region at the same latitude. This indicates that the lake depth in the Nenjiang Member 1–2 epochs was significantly greater than in the Nenjiang Member 3. It was confirmed that the lake level rise in the first two epochs was caused by the rise of the global sea level. This is also supported by the analysis of oxygen isotopes to calculate reliable Paleolake levels.

Table 6. Calculated paleotemperatures of the depositional environment of the Nenjiang Formation

Sample	Horizon	$\delta^{18}O$, ‰ (PDB)	$d^{18}Ow$, ‰ (PDB)	Formula 1	Formula 2	Average temperature, °C
ZK1489-87	K_2n^3	–9.9	–8.82	21.59	22.84	22.21
ZK1489-84	K_2n^3	–10.2	–8.82	22.94	23.91	23.43
ZK1489-81	K_2n^3	–7.3	–8.82	10.82	13.72	12.27
ZK1489-72	K_2n^3	–9.5	–8.82	19.82	21.41	20.61
ZK1489-62	K_2n^3	–10.6	–8.82	24.79	25.36	25.07
ZK1489-40	K_2n^2	–8.5	–8.82	15.57	17.88	16.72
ZK1489-36	K_2n^2	–8.7	–8.82	16.40	18.58	17.49
ZK1489-24	K_2n^2	–7.8	–8.82	12.75	15.44	14.10
ZK1489-14	K_2n^2	–8.5	–8.82	15.57	17.88	16.72
ZK1489-10	K_2n^1	–9.1	–8.82	18.09	19.99	19.04
ZK1489-1	K_2n^1	–9.5	–8.82	19.82	21.41	20.61

Note: Latitude information is from [25], oxygen isotope information of water interface from [27].

5.5. Open and closed lakes

The analysis of carbon and oxygen isotope variations in modern lake basins of different types was carried out. The characteristics of carbon and oxygen isotopes in open lakes refer rather to their origin from the incoming water (surface runoff, groundwater and rainwater falls on the lake surface) [28]. In this study it was established that there were several other factors affecting carbon and oxygen isotopes, so the contents of $\delta^{13}C$ and $\delta^{18}O$ were disregarded in investigating open lakes. On the other hand, the restriction of evaporation from sealed lakes synchronizes with the evolution of carbon and oxygen isotopes, so $\delta^{13}C$ and $\delta^{18}O$ are well-correlated [29]. Talbot suggested that the coefficients of correlation between $\delta^{13}C$ and $\delta^{18}O$ in a closed basin generally exceed 0.5 [30]. In other words, the better the seal, the higher the correlation. Both positive and negative values of $\delta^{18}O$ have been observed in

closed lakes. We linearly fit the measured $\delta^{13}C$ and $\delta^{18}O$ values and found the correlation to be insignificant, 0.031.

Milliman summarized the characteristics of modern open and closed lake basins [31]. In a coordinate system where the vertical axis is represented by $\delta^{13}C$, the abscissa is represented by $\delta^{18}O$ and the origin is set at 0, the resultant distribution is as indicated in Figure 7. These distribution patterns were validated through studies in Turkana Lake (Kenya), Great Salt Lake (United States) and Heleh Lake (Israel). We found that these patterns were basically consistent with Milliman's distribution pattern. Against this background, the analyses of $\delta^{13}C$ and $\delta^{18}O$ distributions in the Nenjiang Formation revealed that most observations corresponded to the respective findings in a modern open lake basin. In other words, in the Nenjiang epoch the Songliao Basin was an open lake basin, suggesting possible transgression.

Previous researches showed that the distribution of illite and kaolinite from continent to sea is connected with paleosalinity of water [32, 33]. The high illite content and low kaolinite content in the first stage of salinity may be related to the marine transgression. It was further demonstrated that water salinization in the Nenjiang Formation was not caused by occlusion and evaporation from the lake, but happened through the physical connection with the sea.

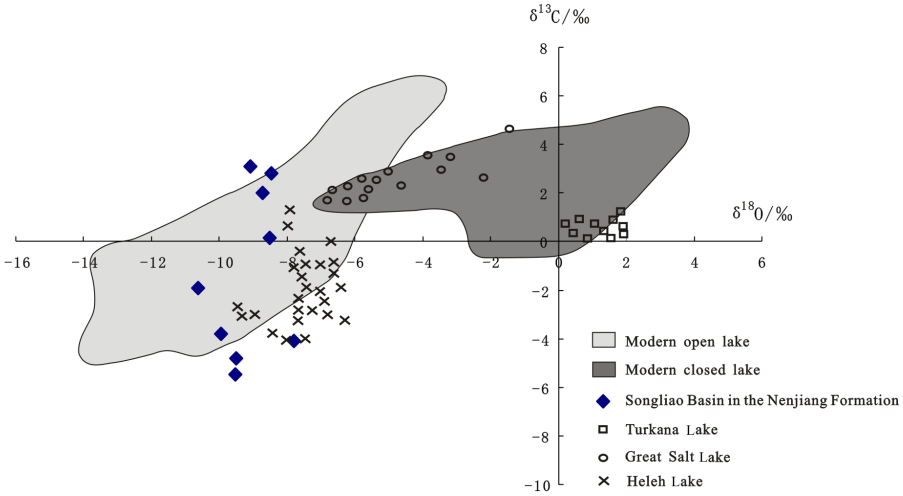

Fig. 7. Correlation between carbon and oxygen isotopes of carbonate minerals in different types of modern lakes [31].

5.6. Productivity of paleolake and enrichment of organic matter

Productivity is defined as the fixed energy rate of a biological energy cycle, and is expressed by the mass of organic matter generated per unit area and per unit time ($g.m^{-2}$ a) [34]. Lake productivity includes both primary and

secondary productivity, although the former is referred to more often. Productivity of paleolakes has typically been measured using organic carbon, isotope and paleontology methods [35, 36].

An important factor for determining the composition of dissolved inorganic carbon isotopes in lake water is the productivity of the lake. When the lake productivity is high, the flourishing phytoplankton absorbs more ^{12}C through photosynthesis, which increases the inorganic carbon content of the surface water, leading to high $\delta^{13}C$ values in native carbonate. Thus, according to compositional changes in the carbon isotope contents of lacustrine carbonate, it is possible to reconstruct changes in paleolake productivity. Based on the results of our study, the average values of $\delta^{13}C$ in the Nenjiang Member 1 and Nenjiang Member 2 are –1.2‰ and 0.225‰, respectively. These values are higher than the $\delta^{13}C$ in the Nenjiang Member 3, –6.68‰. This suggests that the paleolake productivity in Nenjiang Members 1 and 2 was significantly higher than that in the Nenjiang Member 3 as shown by $\delta^{13}C$ values, being almost similar in the first two (Fig. 8).

The progressing transgression tends to result in salinity stratification due to the different salinity of the bottom and upper layers of the lake. Water stratification might be responsible for the improved preservation of organic matter in the first and third stages of salinity. The high salinity phases of Nenjiang Member 1 and the middle Nenjiang Member 2 agreed with peak $\delta^{13}C$ values, indicating that the paleolake achieved maximum productivity in the above two phases. Such conditions are more conducive to the

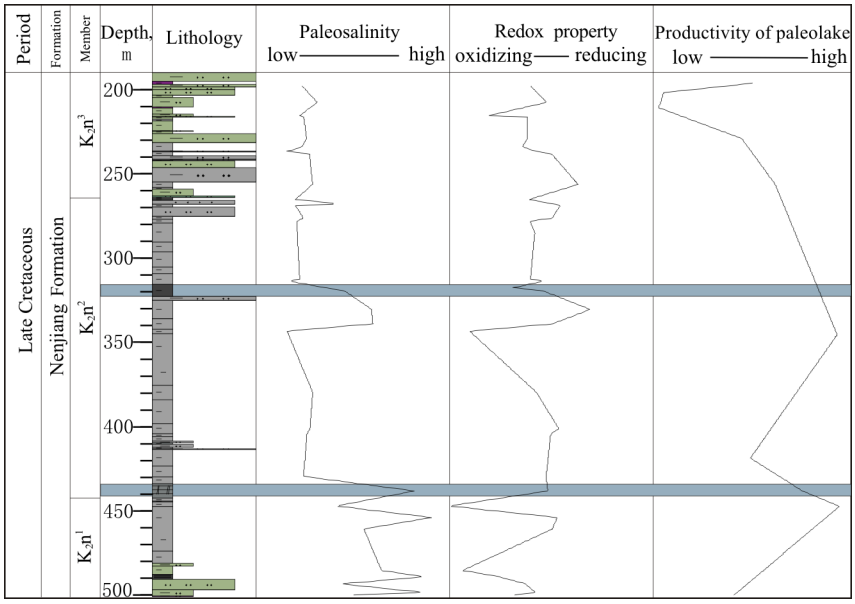

Fig. 8. Paleolimnological characteristics of oil shale enrichment in the Nenjiang Formation.

enrichment of organic matter. Through field observation of drilling cores, as well as oil content tests, two layers of oil shale were found with the respective thicknesses of 8.2 m and 7.5 m. These two layers of the rock represent important landmarks for stratigraphic division in the Nenjiang Formation. The formation and enrichment of oil shale in the Nenjiang Formation took place under three different conditions (Fig. 8): (1) high salinity condition; (2) strongly reducing anaerobic environment, allowing the preservation of organic matter; (3) high lake productivity, allowing plankton to flourish and leading to the formation of productive source rocks.

6. Conclusions

(1) Due to geological transgressive events, the Nenjiang Formation was deposited in a strongly reducing, brackish water environment. Early in the Nenjiang epoch, deposition conditions involved high salinity and a trend from semi-arid and hot towards warm and humid environment that resulted in a decreased salinity at later times. In the middle Nenjiang Member 2, semi-arid and hot climatic conditions led to an increase in salinity. In the late Nenjiang Member 2 and Nenjiang Member 3 epochs, sediments deposition occurred under fluctuating warm and humid to semi-arid and hot conditions with low salinity.
(2) Analysis of paleotemperature records and oxygen isotope patterns revealed that the Nenjiang Formation was deposited in a warm water environment. The paleotemperature of water in the Nenjiang Member 1 and Member 2 was significantly higher than that in the Nenjiang Member 3, which confirms the fact that the rise of the lake level in Nenjiang Member 1 and Member 2 epochs was caused by the global sea-level rise in the Late Cretaceous.
(3) The combined analysis of carbon and oxygen isotopes with clay minerals demonstrated the Songliao Basin to have likely been an open lake during the deposition of the Nenjiang Formation. This is also supported by transgression events.
(4) The paleoenvironment exhibited high productivity and salinity, as well as strongly reducing conditions, which proved to be an ideal environment for enrichment of organic matter.

REFERENCES

1. Yang, Q. C., Jochum, K. P., Stoll, B., Weis, U., Börner, N., Schwalb, A., Frenzel, P., Scholz, D., Doberschütz, S., Haberzetti, T., Gleixner, G., Mäusbacher, R., Zhu, L. P., Andreae, M. O. Trace element variability in single ostracod valves as a proxy for hydrochemical change in Nam Co, central Tibet, during the Holocene. *Palaeogeogr. Palaeocl.*, 2014, **399**, 225–235.

2. Zhu, M. Y., Babcock, L. E., Peng, S. C. Advances in Cambrian stratigraphy and paleontology: Integrating correlation techniques, paleobiology, taphonomy and paleoenvironmental reconstruction. *Palaeoworld*, 2006, **15**(3–4), 217–222.
3. Xi, D. P., Li, G., Wan, X. Q., Jing, X., Li, S. Yaojia-lower Nenjiang Formation and lake evolution of southeastern Songliao Basin, NE China. *Acta Palaeontologica Sinica*, 2009, **48**(3), 556–568 (in Chinese with English abstract).
4. Jing, X., Li, S., Xi, D. P., Zhao, J., Wan, X. Q. Late Cretaceous spores and pollen assemblages and paleoclimate record of the Nenjiang Formation in Nong'An, Jilin Province. *Acta Micropalaeontologica Sinica*, 2011, **28**(2), 193–203 (in Chinese with English abstract).
5. Zhao, J. Late Cretaceous palynology (spores, pollen, algae), climate and lacustrine conditions in Songliao Basin. *China University of Geosciences for Doctoral Degree*, 2013, 66–85 (in Chinese with English abstract).
6. Liu, Z. H., Zheng, R. C., Guo, X. Question of Cretaceous transgression event in Songliao Basin. *Xinjiang Petroleum Geology*, 2013, **34**(3), 357–360 (in Chinese with English abstract).
7. Huang, Y. J., Yang, G. S., Gu, J., Wang, P. K., Huang, Q. H., Feng, Z. H., Feng, L. J. Marine incursion events in the Late Cretaceous Songliao Basin: constraints from sulfur geochemistry records. *Palaeogeogr. Palaeocl.*, 2013, **385**, 152–161.
8. Bechtel, A., Jia, J. L., Strobl, S. A. I., Sachsenhofer, R. F., Liu, Z. J., Gratzer, R., Püttmann, W. Palaeoenvironmental conditions during deposition of the Upper Cretaceous oil shale sequences in the Songliao Basin (NE China): Implications from geochemical analysis. *Org. Geochem.*, 2012, **46**, 76–95.
9. Feng, Z. Q., Jia, C. Z., Xie, X. N., Zhang, S., Feng, Z. H., Cross, T. A. Tectonostratigraphic units and stratigraphic sequences of the nonmarine Songliao basin, northeast China. *Basin Res*., 2010, **22**(1), 79–95.
10. Li, S. Q., Chen, F. K., Siebel, W., Wu, J. D., Zhu, X. Y., Shan, X. L., Sun, X. M. Late Mesozoic tectonic evolution of the Songliao basin, NE China: Evidence from detrital zircon ages and Sr-Nd isotopes. *Gondwana Res.*, 2012, **22**(3–4), 943–965.
11. Zhao, K. B., Sun, C. Q. Application of hydrocarbon geochemical exploration technique in natural gas exploration. *Petroleum Geology & Experiment*, 2004, **26**(6), 574–579 (in Chinese with English abstract).
12. Lerman, A. D. I., Gat, J. (eds.). *Physics and Chemistry of Lakes*. Springer-Verlag, Berlin, 1989.
13. Epstein, S., Mayeda, T. Variation of O^{18} content of waters from natural sources. *Geochim. Cosmochim. Ac*., 1953, **4**(5), 213–224.
14. Clayton, R. N., Degens, E. T. Use of carbon isotope analyses of carbonates for differentiating freshwater and marine sediments. *AAPG Bull.*, 1959, **43**(4), 890–897.
15. Keith, M. L., Weber, J. N. Carbon and oxygen isotopic composition of selected limestone and fossils. *Geochim. Cosmochim. Ac.*, 1964, **28**(10–11), 1787–1816.
16. Zhao, X. Y., Luo, J. C., Yang, F. Application of clay mineral study results to hydrocarbon prospecting in Tarim Basin. *Xinjiang Petroleum Geology*, 2005, **26**(5), 570–576 (in Chinese with English abstract).
17. Edzwald, J. K., O'Melia, C. R. Clay distribution in recent estuarine sediments. *Clays and Clay Miner.*, 1975, **23**, 39–44.
18. Xu, C. Study of clay minerals in some salt lakes of China. *Oceanologia et Limnologia Sinica,* 1988, **19**(3), 278–285 (in Chinese with English abstract).

19. Xu, Y. J. Foraminifera and seawater incursion events of the Late Cretaceous Songliao Basin. *China University of Geosciences for Master's Degree*, 2012, **5**, 39–41 (in Chinese with English abstract).
20. Zhang, X., Huang, X. X., Zhang, W. F. Characteristic of sedimentary evolution of Nenjiang Formation in southern Songliao basin. *Journal of Yangtze University (Nat. Sci. Edit.)*, 2010, **3**(7), 165–167 (in Chinese with English abstract).
21. Jones, B., Manning, D. A. C. Comparison of geochemical indices used for the interpretation of palaeoredox conditions in ancient mudstones. *Chem. Geol.*, 1994, **111**, 111–129.
22. Craig, H. The measurement of oxygen isotope paleotemperatures. In: *Stable Isotopes in Oceanographic Studies and Paleotemperatures* (Tongiorgi, E., ed.). Consiglio Nazionale delle Ricerche, Laboratorio di Geologia Nucleare, Pisa, 1965, 161–182.
23. Emrich, K., Ehhalt, D. H, Vogel, J. C. Carbon isotope fractionation during the precipitation of calcium carbonate. *Earth Planet. Sc. Lett.,* 1970, **8**(5), 363–371.
24. Zhang, X. L. Relationship between carbon and oxygen stable isotopes in carbonate rocks and paleosalinity and paleotemperature of seawater. *Acta Sedimentologica Sinica*, 1985, **3**(4), 18–29 (in Chinese).
25. Zheng, S. H., Zheng, S. C. *Geochemical Analysis of Stable Isotopes.* Beijing University Press, 1986, 12–106 (in Chinese).
26. Shen, J. N, Wang, Q. H., He, J. L., Lu, S. F. Estimation of the ancient lake temperature and paleo-climate of the Cretaceous period in the Songliao Basin. *Journal of Jilin University (Earth Science Edition)*, 2008, **38**(6), 946–952 (in Chinese with English abstract).
27. Yang, W. D., Chen, N. S., Ni, S. J., Nan, J. Y., Wu, M. Q., Jiang, J. Y., Ye, J. L., Feng, X. X., Ran, Y. Carbon and oxygen isotopic composition of carbonate rocks and dinosaur eggshell and environment significance in Cretaceous red layer. *Chinese Science Bulletin*, 1993, **38**(23), 2161–2163 (in Chinese with English abstract).
28. Zhao, Z. Y., Zhao, J. H., Wang, H. J., Liao, J. D., Liu, C. M. Distribution characteristics and applications of trace elements in Junggar Basin. *Natural Gas Exploration and Development,* 2007, **2**, 30–40 (in Chinese with English abstract).
29. Liu, C. Z., Zhao, Q. H., Wang, P. X., Lacustrine carbonate oxygen and carbon isotope correlation and oil paleolimnological type. *Geochemistry*, 2001, **30**(4), 363–367 (in Chinese with English abstract).
30. Talbot, M. R. A review of the palaeohydrological interpretation of carbon and oxygen isotopic ratios in primary lacustrine carbonates. *Chem. Geol. (Isot. Geosci. Sect.)*, 1990, **80**(4), 261–279.
31. Milliman, J. D. (ed.). *Recent Sedimentary Carbonates, Part 1. Marine Carbonates*. Springer, Berlin, 1974**.**
32. Wu, Y. Y., Chen, Z. Y., Wang, Z. H. Distribution of clay minerals in the Yangtze Delta Plain and its paleoenvironmental implication. *Journal of East China Normal University (Natural Science),* 2005, **1**, 92–98 (in Chinese with English abstract).
33. Luo, Z., Shao, L. Y., Yao, G. H., Deng, G. M., Wang, H., Han, J. Mudstones in the Upper Permian coal-bearing series in eastern Yunnan and western Guizhou: Clay minerals composition and their environmental significance. *Journal of Palaeogeograpy*, 2008, **10**(3), 297–304 (in Chinese with English abstract).

34. Wang, P. X. *Introduction to Palaeo-oceanography*. Tongji University Press, Shanghai, 1989, 1–20 (in Chinese).
35. Müller P. J., Suess, E. Productivity, sedimentation rate and sedimentary organic matter in the oceans. I. Organic carbon preservation. *Deep-Sea Res. Pt. I*, 1979, **26**(12), 1347–1362.
36. Mix, A. C. Pleistocene paleoproductivity evidence from organic carbon and foraminiferal species. In: *Productivity of the Oceans: Present and Past* (Berger, W. H., Smetacek, V. S., Wefer, G., eds.). John Wiley and Sons, New York, 1989, 313–340.

Presented by K. Kirsimäe
Received September 9, 2013